Available online at www.sciencedirect.com
ScienceDirect
Trans. Nonferrous Met. Soc. China 25(2015) 2653−2660
Transactions of Nonferrous Metals Society of China
www.tnmsc.cn

Preparation of fibrous nickel powder by precipitation transformation coupled with thermal decomposition

Jian-hui WU, Gang LIU, Tao SU, Wen-hong ZHANG, Mei-mei LUO, Tao WEI

School of Metallurgy and Environment, Central South University, Changsha 410083, China

Received 27 October 2014; accepted 29 December 2014

Abstract: Fibrous particulate precursor was obtained by precipitation transformation in the ternary solution system of ammonium oxalate, nickel chloride and ammonia. The composition and morphology of precursor were characterized by XRD, SEM, IR and DTA/TGA analyses. The results show that the chemical composition and morphology of precursor precipitates at pH=8.4−8.8 are different from those of precursor precipitates at pH=6.0, and the mechanisms of the thermal decomposition of the precursors are different. The effects of various conditions in the process of thermal decomposition, including precursor morphology, atmosphere, temperature and time on the morphology and dispersion degree of obtained nickel powders were studied in detail. The final product inherits the morphology of precursor when the thermal decomposition is conducted under a weakly reducing atmosphere at temperature range of 400−440 °C for 30 min. Fibrous nickel powder can be produced with good dispersion, and its shape changes from smooth, straight and compact fiber into loose and curved fiber with rough surface.

Key words: precursor; fibrous nickel powder; precipitation transformation; thermal decomposition

1 Introduction

In recent years, nickel nanoparticles have attracted increasing attention because of their unique properties, which were applied in magnetic devices [1], catalysts [2], batteries [3], electrochromic devices [4], fuel cells [5], microwave absorber and electromagnetic (EM) shielding material [6]. Especially, one-dimensional (1D) nickel nanoparticles are investigated by many scientists due to their distinctive geometry characteristics and novel chemical and physical properties such as size effect, shape anisotropy, dipolar interaction and magnetization effect. Many novel techniques have been employed to synthesize quasi 1D nickel nanoparticles including template [7], liquid-phase reduction [8], electro-deposition [9], sol−gel−thermal decomposition [10]. The template methods have been widely employed to synthesize magnetic metal micro/nanofibres and wires. Many magnetic metal fibres were synthesized by using porous anodic aluminum oxide (AAO) or polycarbonate membrane as the template [7,11]. However, this method has a somewhat complicated process and results in a low yield. Carbon nanotube (CNT) is another excellent template for the preparation of magnetic metal fibre. M-CNT (M denotes magnetic metals and their alloys) have attracted great interests and were used as EM absorbing materials [12,13]. However, the addition of nonmagnetic carbon will lead to a decrease of permeability [14].

The pure solid nickel oxalate has been studied by many scientists [15]. The researches aimed to prepare spherical nickel powders at low pH value. In the previous researches, fibrous cobalt and copper powders were prepared by the precipitation−thermal decomposition method [16,17]. Through a series of experiments, it is found that this method is also adapted to the preparation of nickel powder. In contrast to other methods, this method has the advantages such as simple process, low cost, controllable morphology and good quality of the products. For this method, once the particles with special morphology are formed, their basic characteristics, such as morphology, will be maintained. In this study, the preparation of fibrous nickel powder was investigated by precipitation transformation in Ni^{2+}−NH_3−$C_2O_4^{2-}$−H_2O system coupled with thermal decomposition. The mechanisms of precursor preparation and thermal decomposition of precursor were

Foundation item: Project (2010FJ3012) supported by the Science and Technology Plan Foundation of Hunan Province, China
Corresponding author: Jian-hui WU; Tel: +86-13808482782; E-mail: wujianhui218@163.com
DOI: 10.1016/S1003-6326(15)63888-2

discussed. The effects of experiment conditions on the composition, size and morphology of product during the process of precursor preparation and thermal decomposition were studied in detail.

2 Experimental

2.1 Preparation of precursor

All the chemicals are analytical grade and were used without further purification. All solutions were freshly prepared before each reaction. First, 0.06 mol $NiCl_2·6H_2O$ was dissolved in 100 mL deionized water labeled as solution I, and 0.072 mol $(NH_4)_2C_2O_4$ was dissolved in 100 mL deionized water labeled as solution II. Then, solution I was injected into solution II by a peristaltic pump at a rate of 2.5 mL/min, and the temperature was controlled at 65 °C in a water bath. After 15 min agitation, ammonia solution was added into the light green suspension to adjust and stabilize the pH values at 6.0, 7.5, 8.4 and 8.8, respectively. After agitating and aging, the precipitate was washed with distilled water followed by ethanol and acetone for three times. Then the precipitate was filtered and dried in a vacuum drier at 100−120 °C for more than 12 h.

2.2 Preparation of nickel powder

The dried precursor powders were decomposed in a tubular electric furnace under a mixed atmosphere of nitrogen and hydrogen at temperatures of 360−480 °C for 15−60 min. The final nickel powders were produced after a proper surface treatment to avoid spontaneous combustion in the air.

2.3 Characterization

The X-ray diffraction (XRD) patterns of the products were recorded on an X-ray diffractometer (D/max rA10, Japan) using Cu K_α radiation (λ=0.15406 nm). The morphologies of samples were studied on a JSM−5600LV scanning electron microscope at 20 kV. The thermal studies were conducted on a DuPont 9900 thermal analyzer under pure argon atmosphere at a heating rate of 10 °C/min. The infrared (IR) spectra were recorded on a Nexus 470 spectrometer in the range of 4000−400 cm^{-1}, and the spectra were measured on KBr discs.

3 Results and discussion

3.1 precipitation transformation

3.1.1 Precursors synthesized at different pH values

Figure 1 illustrates the X-ray diffraction patterns of precursor samples obtained at different transformation pH values. As shown in Fig. 1, the peak positions of precursor particles obtained at pH value of 6 are consistent with standard JCPDS card of $NiC_2O_4·2H_2O$, which means that the obtained precursor is $NiC_2O_4·2H_2O$ at pH value of 6, while the other three X-ray diffraction patterns are quiet different from it. By comparing the peak positions of precursors obtained at pH values of 8.4 and 8.8, it can be found that they are basically the same, meaning that the obtained precursor is tending to an equilibrium state.

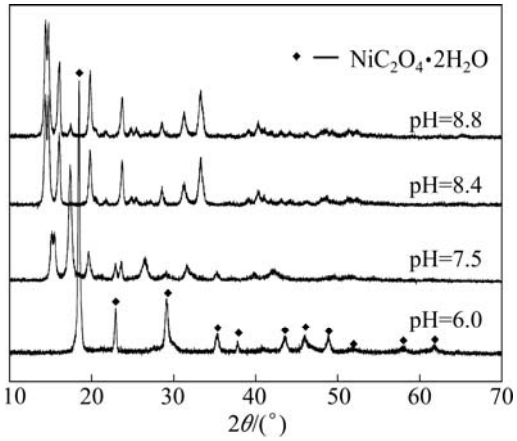

Fig. 1 XRD patterns of precursor particles

Figure 2 shows the SEM images of precursor samples synthesized at different pH values. As shown in Fig. 2, pH value plays an important role on the formation of fibrous morphology. When pH value is low, the obtained powders are spherical crystals. With increasing the pH value of Ni^{2+}−NH_3−$C_2O_4^{2-}$−H_2O system, nickel oxalates with different contents of ammonia precipitate, can be confirmed by the IR spectra analysis in Fig. 3. Due to the composition concentration fluctuation in the feeding process, the nascent precipitate is a mixture of nickel oxalates containing different contents of ammonia. During aging, since different contents of ammonia may lead to different solubilities of the nickel oxalates, according to the dissolution−recrystallization mechanism, the compounds with high solubility dissolve into the solution, which provides a continuous supply of material of crystal growth for the compounds with low solubility. Under this low supersaturation condition, it is beneficial for the growth of long fibrous particles. When pH value ranges from 8.4 to 8.8, the particles turn to be obviously fibrous with satisfactory dispersion, and the optimum ratio in axis/diameter is from 15 to 20.

3.1.2 IR spectra of precursors at different pH values

The IR spectra of as-prepared precursor samples at various pH values are shown in Fig. 3. In spectrum curve (a), the band at 3390 cm^{-1} is attributed to the symmetrical stretching vibration of hydrogen bond of $C_2O_4^{2-}$ ions, the band at 1622 cm^{-1} is due to the stretching vibrations absorption mode of $C_2O_4^{2-}$. In the

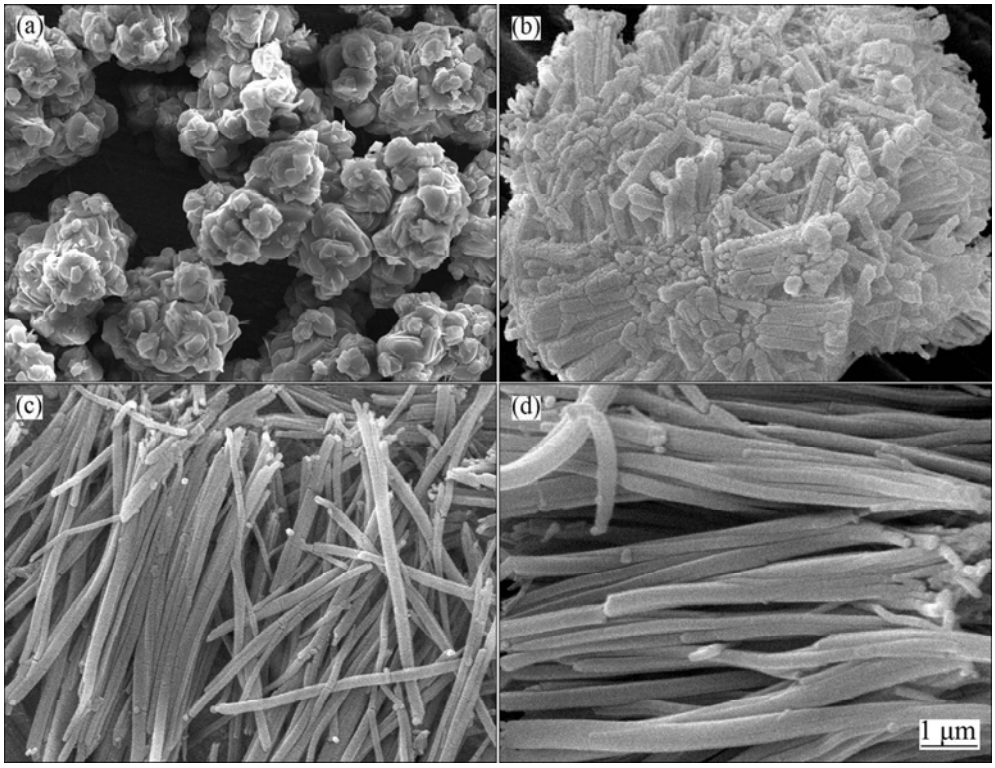

Fig. 2 SEM micrographs of precursor powders prepared at different pH values: (a) 6.0; (b) 7.5; (c) 8.4; (d) 8.8

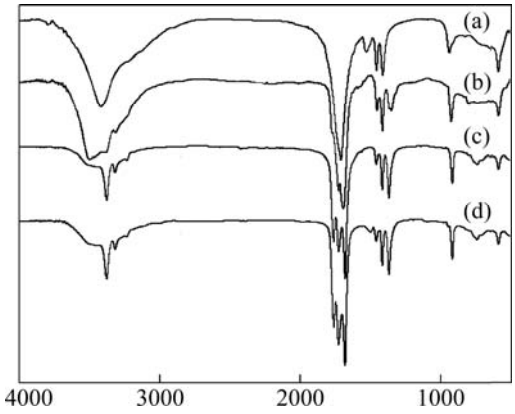

Fig. 3 IR spectra of precursor particles prepared at different pH values: (a) 6; (b) 7.5; (c) 8.4; (d) 8.8

range of 1450−1300 cm^{-1}, there are a weak band at 1434 cm^{-1} and two strong bands at 1360 and 1315 cm^{-1} resulting from the vibrations of $C_2O_4^{2-}$. In the range of 824−490 cm^{-1}, the weak band at 824 cm^{-1} is attributed to the vibration mode of $C_2O_4^{2-}$ and the strong one at 490 cm^{-1} is originated from the stretching vibrations of Ni—O bond. The above analysis is consistent with Ref. [18]. The IR spectrum curve (b) differs from curve (a), a band at 3473 cm^{-1} is the band shifted from 3390 cm^{-1} and the intensity become less. The shoulder at 1622 cm^{-1} band splits into the shoulder 1641 and 1607 cm^{-1} which are attributed to the bending vibration mode of NH_3. In the range of 1450−1210 cm^{-1}, there are three stretching vibrations of $C_2O_4^{2-}$, and the shoulder at 1434 cm^{-1} disappears and a band at 1251 cm^{-1} appears. In the range of 824−490 cm^{-1}, the bands at 824 and 490 cm^{-1} are still the same as those of curve (a). Compared with curve (a), curve (c) has some changes as follows: The band at 3390 cm^{-1} splits into 3348 and 3285 cm^{-1}. The shoulder at 1622 cm^{-1} splits into three bands at 1677, 1643 and 1592 cm^{-1}, of which the bands at 1677 and 1592 cm^{-1} are attributed to the bending vibrations of NH_3. There are three stretching vibrations of $C_2O_4^{2-}$ (1361, 1318 and 1271 cm^{-1}), and one wagging vibration of H_2O molecule (1402 cm^{-1}) between the bands at 1450 and 1210 cm^{-1}. In the range of 824−490 cm^{-1}, the weak stretching vibration of $C_2O_4^{2-}$ at 619 cm^{-1} appears. Curve (d) is the same as curve (c) except absenting one weak band at 1402 cm^{-1}, which can be assigned to the wagging vibrations of H_2O molecule. According to the above analysis, the results show that as-prepared precursor particles are $NiC_2O_4{\cdot}2H_2O$ when the pH value is 6.0, with the pH value going up, more ammonia begin to react with precursor, thus the composition of precursor powder consists of ammonia and nickel oxalate instead of pure nickel oxalate.

3.1.3 TGA and DTA analysis of precursor

The TGA/DTA curves of the precursor samples synthesized at different pH values are shown in Fig. 4. Figure 4(a) shows that DTA curve of the precursor samples synthesized at pH=6.0 has only two DTA peaks

in the range of 100−500 °C. The peak in the range of 200−250 °C corresponds to the dehydration peak of pure $NiC_2O_4·2H_2O$ and the mass loss in the TGA curve is 19.15%. The second peak of DTA curve occurs about at 360 °C, which corresponds to the decomposition peak of pure NiC_2O_4 and the mass loss in the corresponding TGA curve is 53.10%. The temperature ranges of dehydration and decomposition and the total mass loss of the precursor synthesized at pH=6.0 are accordant with those of the pure $NiC_2O_4·2H_2O$. Figure 4(b) shows that the DTA/TGA curves of precursors synthesized at pH=8.4 are different from those shown in Fig. 4(a). From the DTA/TGA curves shown in Fig. 4(b), it can be seen that between 60 and 150 °C, there is a narrow endothermic peak in the DTA curve, and in the corresponding range of temperature, the sample has a mass loss of about 16.15%, which is the removal of NH_3 in the precursor. In the range of 210−300 °C, there appears a wider endothermic peak in the DTA curve with the corresponding mass loss of 8.79%, which is attributed to the removal process of crystallization water in the precursor. The sharp endothermic peak between 320 and 400 °C and the mass loss of about 47.8% are due to the decomposition of NiC_2O_4. When the temperature is higher than 400 °C, the TGA curve has a slight ascension which possibly

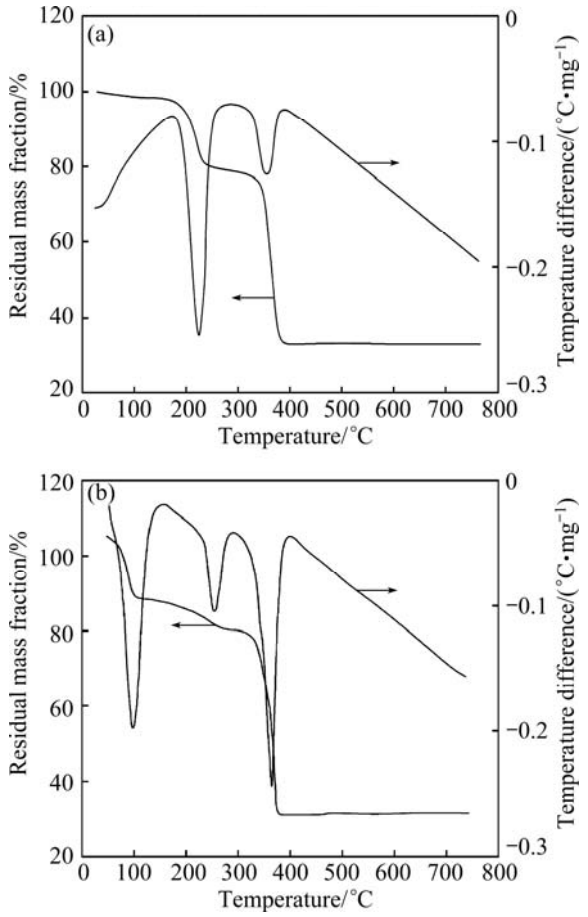

Fig. 4 TGA/DTA curves of precursors synthesized at different pH values: (a) 6.0; (b) 8.4

because of the impurity of the argon, which contains little oxygen that oxidized the nickel powder at high temperature. To prevent the oxidation of nickel powder in high temperature, a reducing atmosphere was applied in the experiment.

Based on the analyses results of the precursor powders by XRD, IR spectra and TGA/DTA thermodynamic analysis, it can be found that the precipitate transforms from pure nickel oxalate to complex nickel oxalate with increasing the pH value. The formula of complex nickel oxalate can be expressed as $NiC_2O_4·xNH_3·yH_2O$, where x and y represent the mole numbers of components which depend on the solution pH value, concentration of ammonia and drying temperature. Of course, the x and y values need to be studied further.

According to the results of TGA/DTA, the mechanism of the thermal decomposition of complex nickel oxalate can be expressed as follows:

The first stage is the deamination:

$$NiC_2O_4·xNH_3·yH_2O=NiC_2O_4·yH_2O+xNH_3↑$$

The second stage is the dehydration:

$$NiC_2O_4·yH_2O=NiC_2O_4+yH_2O↑$$

The last stage is the decomposition of nickel oxalate:

$$NiC_2O_4=Ni+2CO_2↑$$
$$NiC_2O_4=NiO+CO↑+CO_2↑$$

The last stage decides the necessity of keeping the reducing atmosphere in the thermal decomposition process.

3.2 Effects of thermal decomposition conditions on morphology of nickel powder

3.2.1 XRD analysis

The thermal decomposition is conducted under a weakly reducing atmosphere at the respective temperatures of 360, 400, 440, 480 °C for 30 min. The X-ray diffraction patterns of the final products are shown in Fig. 5. By comparing the positions with standard JCPDS card of face-centered cubic nickel, it is found that they are quite consistent, meaning that the final product is face-centered cubic nickel. By comparing the X-ray diffraction patterns, it can be found that, with raising the decomposition temperature, the diffraction peaks get sharper and the interplanar spacing increases, which means that the final products obtained under a high temperature have better crystallinity. It is generally known that a high decomposition temperature may lead to agglomeration problems of ultrafine powder, while a low decomposition temperature may lead to incomplete decomposition of precursor. So the choice of decomposition temperature is very important.

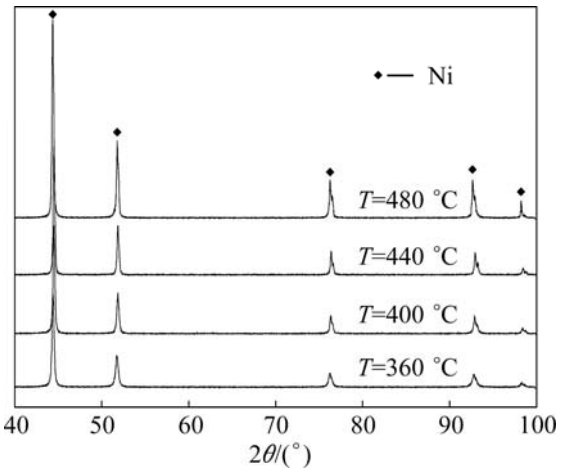

Fig. 5 XRD patterns of final products

3.2.2 Effect of precursor morphology

Figures 6(a) and (c) show the SEM micrographs of two different precursor particles, Figs. 6(b) and (d) show the SEM micrographs of the nickel powder samples obtained from the thermal decomposition corresponding to Figs. 6(a) and (c), respectively. The thermal decomposition is conducted under a weakly reducing atmosphere at the temperature of 400 °C for 30 min. As shown in Fig. 6, the morphology of precursor has a decisive effect on that of nickel powder after thermal decomposition. Through the comparison, it comes to the conclusion that after decomposition, the grain diameter of extremely small precursor powders become much larger and the powders agglomerate seriously with gas holes between particles. However, the fibrous precursor particles with good dispersion keep fibrous with good dispersion after decomposition, meaning that the final product inherits the morphology of precursor. It can be concluded that the precursor samples shown in Fig. 6(a) are not suitable for the preparation of high quality nickel powders, but the well dispersed, distinct fibrous precursor powders do. In following investigation, the complex nickel oxalate containing ammonia with fibrous morphology is selected as the precursor for preparing the fibrous nickel powder by decomposition.

3.2.3 Effect of decomposition atmosphere

Figure 7 shows the SEM micrographs of nickel powder samples obtained under different reducing atmospheres at temperature of 400 °C for 30 min, from which, it can be found that the particles obtained under a weakly reducing atmosphere are fibrous and porous with good dispersion. With increasing the fraction of H_2, the reduction reaction dominates increasingly, which accelerates the reaction rate, and the obtained particles arrange closely and sintering occurs. It comes to the conclusion that a weakly reducing atmosphere is necessary for the decomposition.

3.2.4 Effect of decomposition temperature

Figure 8 shows the SEM micrographs of nickel

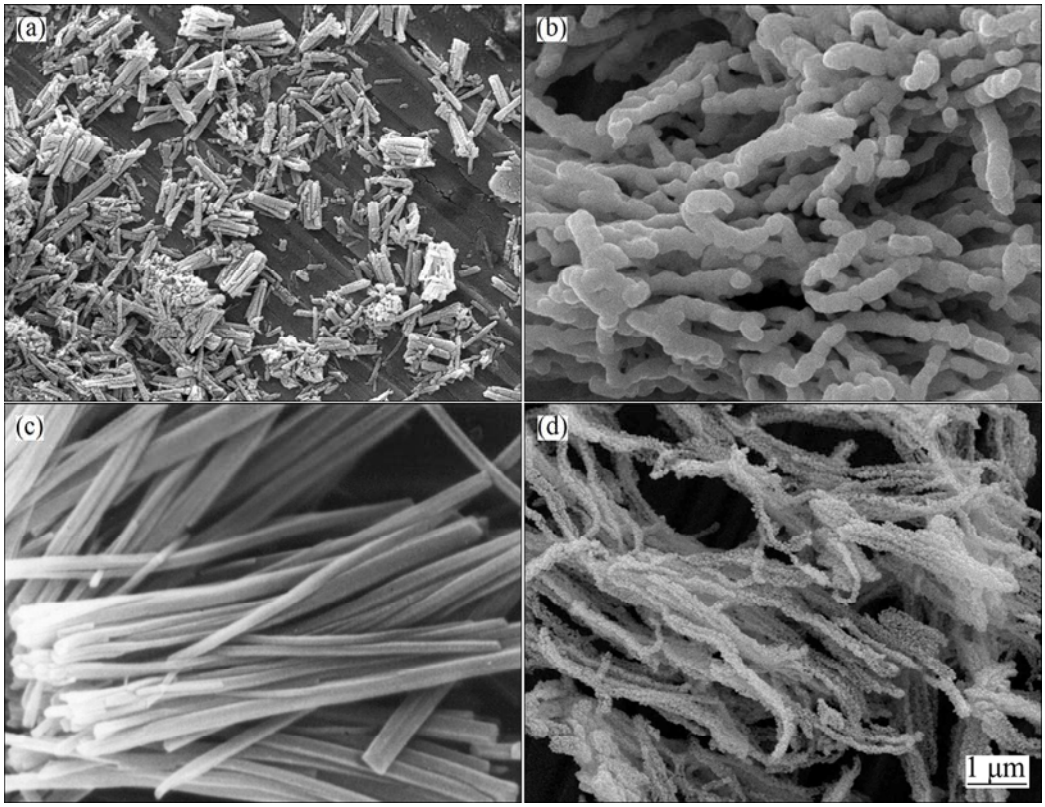

Fig. 6 SEM micrographs of various precursors (a, c) and nickel powders after thermal decomposition (b, d)

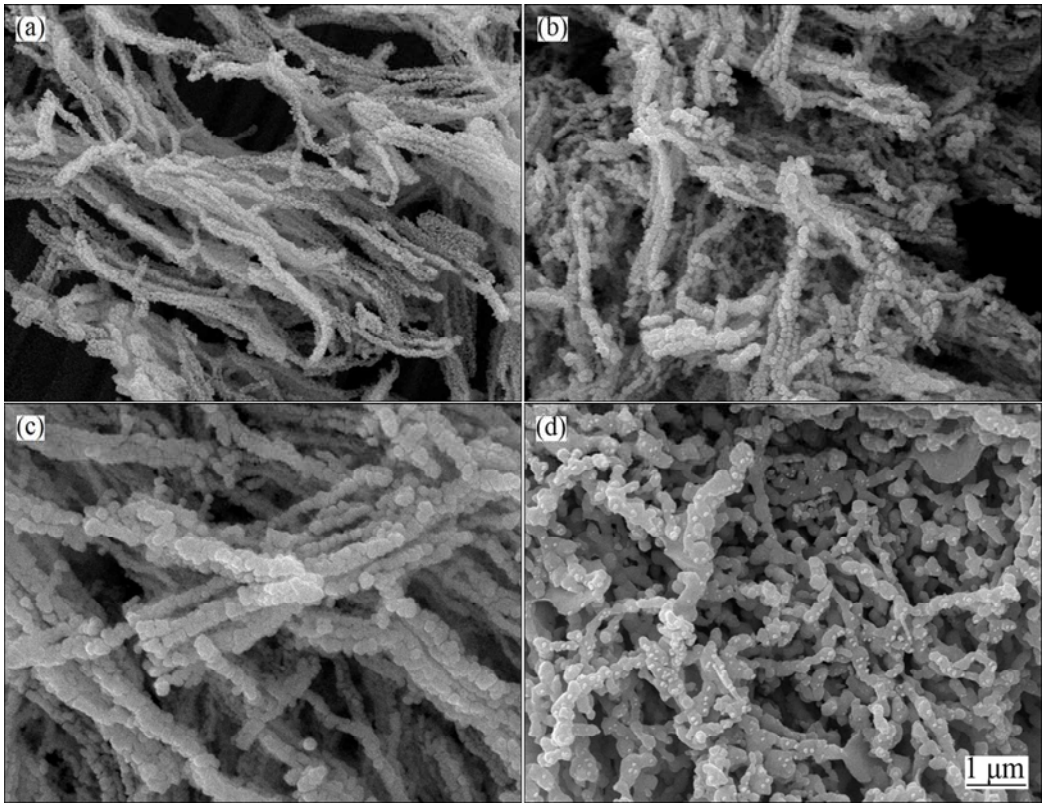

Fig. 7 SEM micrographs of nickel powders obtained under various decomposition atmospheres: (a) 10% H_2 + 90% N_2; (b) 20% H_2 + 80% N_2; (c) 30% H_2 + 70% N_2; (d) 40% H_2 + 60% N_2

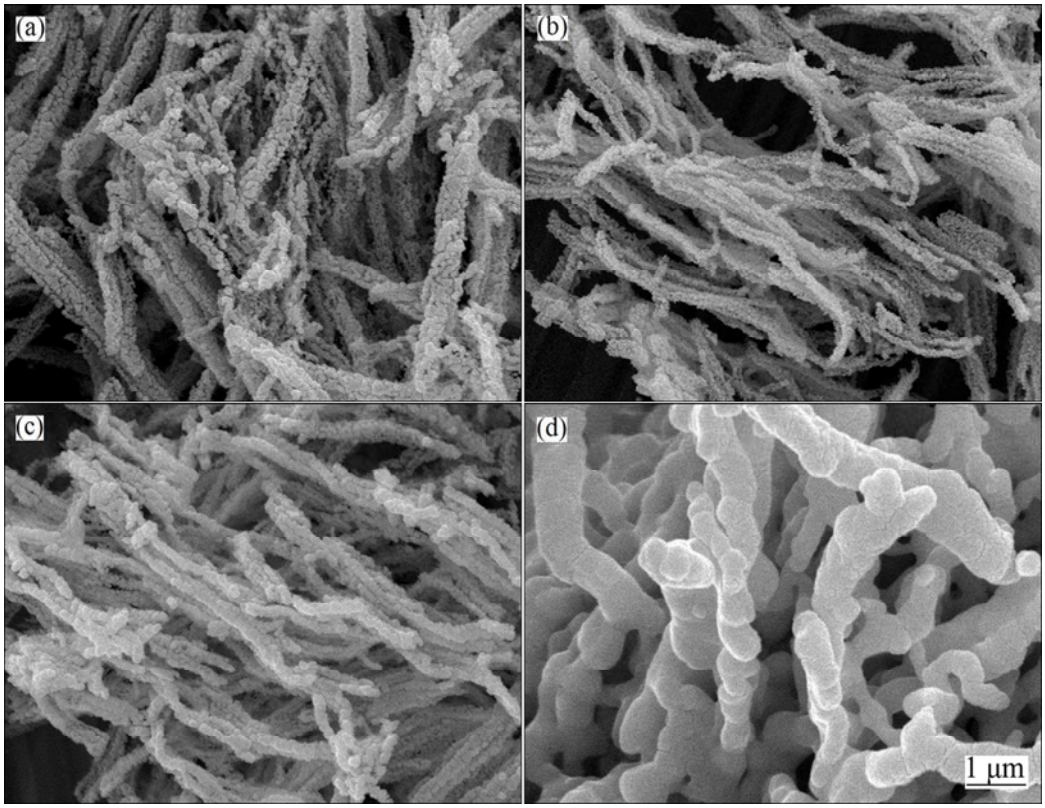

Fig. 8 SEM micrographs of nickel powders obtained under various decomposition temperatures: (a) 360 °C; (b) 400 °C; (c) 440 °C; (d) 480 °C

powder samples obtained by decomposing under a weakly reducing atmosphere and at the temperatures of 360, 400, 440 and0 480 °C, respectively, with a duration of 30 min. As the thermal decomposition of precursor includes deamination, dehydration and decomposition stages, under a certain temperature, there are large quantities of gases release from the solids at each stage, which makes the obtained product porous and loose. At temperature range of 400−440 °C, the gases release slowly which results in ordering decomposition reaction, and the final product inherits the morphology of precursor. Fibrous nickel powder can be produced with good dispersion, and its shape changes from smooth, straight and compact fiber into loose and curved fiber with rough surface. It comes to the conclusion that the optimum decomposition temperature ranges from 400 to 440°C.

3.2.5 Effect of decomposition time

Figure 9 shows the SEM micrographs of nickel powder samples obtained under a weakly reducing atmosphere at temperature of 400 °C for different decomposition time. It can be found that the powders are definitely fibrous and well disperse after decomposition for 15−30 min. While a much longer decomposition time leads to significant aggregation of nickel particles, the longer the decomposition time, the severer the agglomeration. So the optimum decomposition time is 30 min.

4 Conclusions

1) The precipitation precursor is complex nickel oxalate containing ammonia and the formula can be expressed as $NiC_2O_4{\cdot}xNH_3{\cdot}yH_2O$, where x and y represent the mole numbers of components which depend on the solution pH value, concentration of ammonia and drying temperature. The mechanism of the thermal decomposition of complex nickel oxalate can be inferred as deamination, dehydration and decomposition of nickel oxalate.

2) The final product keeps the morphology of precursor. When the thermal decomposition is conducted under a weakly reducing atmosphere at temperature range of 400−440 °C for 30 min, fibrous nickel powder can be produced with good dispersion, and its shape changes from smooth, straight and compact fiber into loose and curved fiber with rough surface.

3) The crucial point for the formation of fibrous precursor is to yield complex nickel oxalate containing ammonia. The complex is formed via the reaction of nickel oxalate suspension and ammonia, in which the suspension results from the reaction of oxalate and nickel ions.

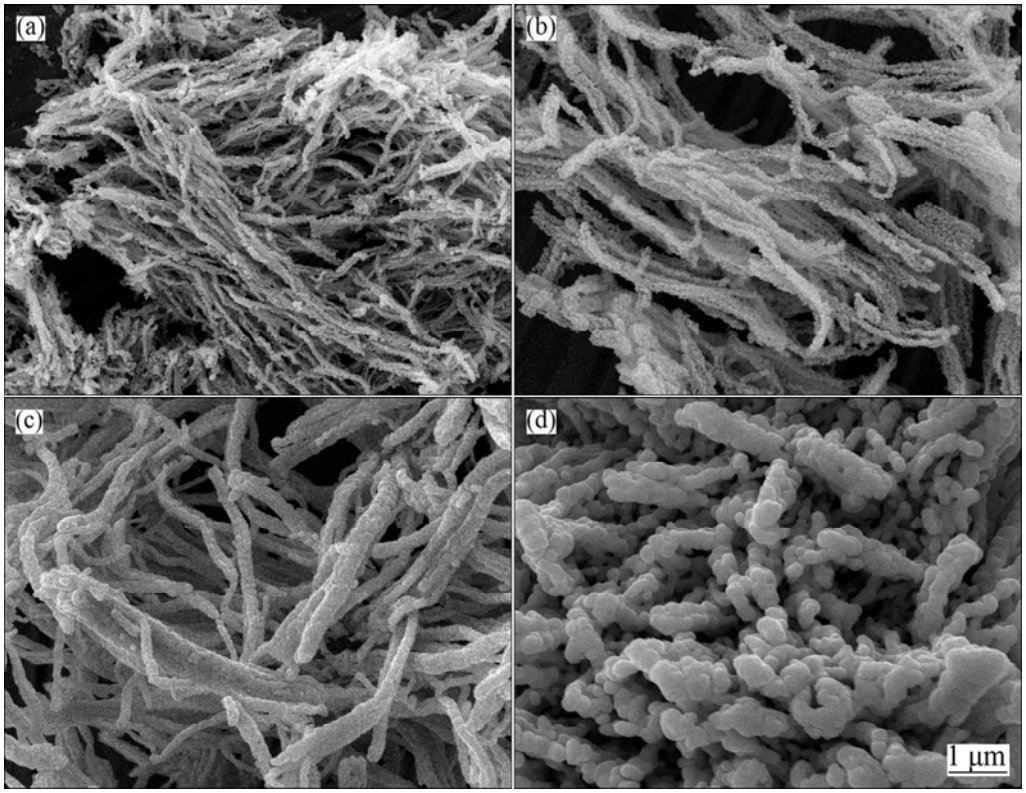

Fig. 9 SEM micrographs of nickel powders obtained under various decomposition time: (a) 15 min; (b) 30 min; (c) 45 min; (d) 60 min

References

[1] KNECHT M R, GARCIA-MARTINEZ J C, CROOKS R M. Synthesis, characterization, and magnetic properties of dendrimer-encapsulated nickel nanoparticles containing <150 atoms [J]. Chemistry of Materials, 2006, 18(21): 5039−5044.

[2] ZHANG You-xian, FU Wen-jie, AN Xue-qin. Preparation of nickel nanoparticles in emulsion [J]. Transactions of Nonferrous Metals Society of China, 2008, 18(1): 212−216.

[3] SHUKLA A K, VENUGOPALAN S, HARIPRAKASH B. Nickel-based rechargeable batteries [J]. Journal of Power Sources, 2001, 100(1): 125−148.

[4] NEIVA E G C, BERGAMINI M F, OLIVEIRA M M, MARCOLINO JR L H, ZARBIN A J G. PVP-capped nickel nanoparticles: Synthesis, characterization and utilization as a glycerol electrosensor [J]. Sensors and Actuators B: Chemical, 2014, 196: 574−581.

[5] TEHRANI R M A, AB GHANI S. The nanocrystalline nickel with catalytic properties on methanol oxidation in alkaline medium [J]. Fuel Cells, 2009, 9(5): 579−587.

[6] BAI Liu-yang, YUAN Fang-li, TANG Qing. Synthesis of nickel nanoparticles with uniform size via a modified hydrazine reduction route [J]. Materials Letters, 2008, 62(15): 2267−2270.

[7] GAO Bo, QIAO Liang, WANG Jian-bo, LIU Qing-fang, LI Fa-shen, FENG Jie, XUE De-sheng. Microwave absorption properties of the Ni nanowires composite [J]. Journal of Physics D: Applied Physics, 2008, 41(23): 235005.

[8] WANG Da-peng, SUN Dong-bai, YU Hong-ying, QIU Zhi-gang, MENG Hui-min. Preparation of one-dimensional nickel nanowires by self-assembly process [J]. Materials Chemistry and Physics, 2009, 113(1): 227−232.

[9] LEE J K, YI Y, LEE H J, UHM S, LEE J. Electrocatalytic activity of Ni nanowires prepared by galvanic electrodeposition for hydrogen evolution reaction [J]. Catalysis Today, 2009, 146(1): 188−191.

[10] YANG Xiao-jiao, LIU Ying, LI Jun, ZHANG Xiao-yan. Study on the thermal decomposition of nickel fibers prepared by nickel citrate [J]. Journal of Functional Materials, 2011, 42(8): 1474−1477. (in Chinese)

[11] CHEN Po-chun, CHANG Yun-min, WU Pu-wei, CHIU Yu-fan. Fabrication of Ni nanowires for hydrogen evolution reaction in a neutral electrolyte [J]. International Journal of Hydrogen Energy, 2009, 34(16): 6596−6602.

[12] SRIVASTAVA R K, NARAYANAN T N, MARY A P R, ANANTHARAMAN M R, SRIVASTAVA A, VAJTAI R, AJAYAN P M. Ni filled flexible multi-walled carbon nanotube–polystyrene composite films as efficient microwave absorbers [J]. Applied Physics Letters, 2011, 99(11): 113116.

[13] LV R T, KANG F Y, GU J L, GUI X C, WEI J Q, WANG K L, WU D H. Carbon nanotubes filled with ferromagnetic alloy nanowires: Lightweight and wide-band microwave absorber [J]. Applied Physics Letters, 2008, 93(22): 223105.

[14] LIU J R, ITOH M, TERADA M, HORIKAWA T, MACHIDA K I. Enhanced electromagnetic wave absorption properties of Fe nanowires in gigaherz range [J]. Applied Physics Letters, 2007, 91(9): 093101.

[15] CARNEY C S, GUMP C J, WEIMER A W. Rapid nickel oxalate thermal decomposition for producing fine porous nickel metal powders. Part 1: Synthesis [J]. Materials Science and Engineering A, 2006, 431(1): 1−12.

[16] ZHAN Jing, LIU Rong-yi, ZHANG Chuan-fu, FAN You-qi, DONG Cheng-yong. Shape-controlled synthesis of porous fibrous cobalt powders [C]//EPD congress of Minerals, Metal and Materials. San Francisco: The Minerals, Metals and Materials Society, 2009: 55−65.

[17] FAN You-qi, ZHANG Chuan-fu, WU Jian-hui, ZHAN Jing, YANG Ping. Composition and morphology of complicated copper oxalate powder [J]. Transactions of Nonferrous Metals Society of China, 2010, 20(1): 165−170.

[18] GARCIA-CLAVEL M E, MARTINEZ-LOPE M J, CASAIS-ALVAREZ M T. Thermal study of $NiC_2O_4{\cdot}2H_2O$ obtained by a solid state reaction at room temperature and normal pressure [J]. Thermochim Acta, 1987, 118: 123−134.

沉淀转化–热分解法制备纤维状镍粉

邬建辉，刘 刚，苏 涛，张文宏，罗妹妹，魏 涛

中南大学 冶金与环境学院，长沙 410083

摘 要：以氯化镍、草酸铵和氨水为原料，通过沉淀转化制备纤维状前驱体。采用 XRD、SEM、IR 和 DTA/TGA 分析手段研究前驱体粉末的成分与形貌。结果表明：在 pH=8.4~8.8 时得到的前驱体在形貌和成分等方面均不同于在 pH=6.0 得到的前驱体，且两种条件下所得前驱体热分解的机理也不同。研究前驱体形貌、热分解气氛、温度及时间对镍粉形貌及分散性的影响，发现前驱体粉末在弱还原性气氛、温度为 400~440°C 下分解 30 min 时，最终产品基本保持前驱体的形貌。得到的纤维状镍粉分散性良好，但每根纤维表面不再光滑，而是具有大量微孔的粗糙形态。

关键词：前驱体；纤维状镍粉；沉淀转化；热分解

(Edited by Mu-lan QIN)